A Dedicated Neonatal Brain Imaging System

Emer J. Hughes,[1]* Tobias Winchman,[2] Francesco Padormo,[1] Rui Teixeira,[1] Julia Wurie,[1] Maryanne Sharma,[1] Matthew Fox,[1] Jana Hutter,[1] Lucilio Cordero-Grande,[1] Anthony N. Price,[1] Joanna Allsop,[1] Jose Bueno-Conde,[1] Nora Tusor,[1] Tomoki Arichi,[1] A. D. Edwards,[1] Mary A. Rutherford,[1] Serena J. Counsell,[1] and Joseph V. Hajnal [1]

Purpose: The goal of the Developing Human Connectome Project is to acquire MRI in 1000 neonates to create a dynamic map of human brain connectivity during early development. High-quality imaging in this cohort without sedation presents a number of technical and practical challenges.

Methods: We designed a neonatal brain imaging system (NBIS) consisting of a dedicated 32-channel receive array coil and a positioning device that allows placement of the infant's head deep into the coil for maximum signal-to-noise ratio (SNR). Disturbance to the infant was minimized by using an MRI-compatible trolley to prepare and transport the infant and by employing a slow ramp-up and continuation of gradient noise during scanning. Scan repeats were minimized by using a restart capability for diffusion MRI and retrospective motion correction. We measured the 1) SNR gain, 2) number of infants with a completed scan protocol, and 3) number of anatomical images with no motion artifact using NBIS compared with using an adult 32-channel head coil.

Results: The NBIS has 2.4 times the SNR of the adult coil and 90% protocol completion rate.

Conclusion: The NBIS allows advanced neonatal brain imaging techniques to be employed in neonatal brain imaging with high protocol completion rates. **Magn Reson Med 78:794–804, 2017.**

Key words: neonatal; brain; head coil; unsedated

INTRODUCTION

The goal of the Developing Human Connectome Project (DHCP) is to use MRI to create a dynamic map of human brain connectivity during an early period of human brain development from 23 to 44 weeks (wk) postconceptual age (PCA). The project will study 1000 neonates including those born preterm. Studying this fragile and inherently uncooperative population presents a number of technical and practical challenges (1,2). Many neonatal research MRI centers perform neonatal brain imaging using adult head coils, which produce suboptimal signal-to-noise ratio (SNR). Dedicated close-fitting receive array coils have been shown to improve SNR in neonatal and pediatric imaging (3). Although these coils provide increased SNR, they create challenges for handling the infant and positioning the head within the smaller space of the neonatal coil. Furthermore, achieving sufficient immobilization of the infant's head and the provision of acoustic protection within the neonatal coil without compromising SNR can also be a major problem. In the past, many studies of neonates employed sedation, which can greatly increase examination completion rates and reduce motion artifact. The use of sedation to image neonates for the purpose of research is becoming increasingly difficult to justify (4–6) and subjects studied within the DHCP will be imaged during natural sleep. In addition, research MRI protocols tend to have relatively longer acquisition times (7) than clinical examinations and high acoustic noise due to the use of high gradient scans such as diffusion MRI (dMRI) increase vulnerability to motion artifacts, which very often lead to early termination of the scan protocol (6).

To acquire high-quality imaging without sedation requires careful consideration of image acquisition, infant handling, monitoring, immobilization, and management of acoustic noise. We therefore specifically designed a neonatal brain imaging system (NBIS) for the DHCP. The system consists of a joint design of a dedicated 32-channel receive array coil and positioning device that allows placement of the infant's head deep into the coil for maximum SNR with minimum disturbance to the infant. Dedicated slim immobilization pieces were developed to hold the infant's head and reduce gross motion without compromising SNR. A key innovation is the development of a transport system that allows the infant to be prepared and sufficiently settled into natural sleep while away from the scanner, then placed in situ for scanning with minimal further disturbance. To facilitate this, a dedicated MRI compatible trolley was developed to transport the positioning device with the infant on board. The positioning device and head coil sit securely on a frame on the scanner bed and are surrounded by an acoustic hood. To further reduce the negative effects of gradient noise, scanner software was modified to create a slow ramp-up and continuation of

[1]Centre for the Developing Brain, Perinatal Imaging and Health, Imaging Sciences and Biomedical Engineering Division, Kings College, London, United Kingdom.

[2]Rapid Biomedical GmbH, Rimpar, Germany.

*Correspondence to: Emer J. Hughes, Centre for the Developing Brian, Perinatal Imaging and Health, Imaging Sciences and Biomedical Engineering Division, Kings College London, 1st Floor South Wing, St. Thomas Hospital, London SE1 7EH, United Kingdom. E-mail, emer.hughes@kcl.ac.uk

Received 5 April 2016; revised 16 August 2016; accepted 20 August 2016

DOI 10.1002/mrm.26462

Published online 19 September 2016 in Wiley Online Library (wileyonlinelibrary.com).

Table 1
Design Considerations for Each Element of the NBIS

1. Head coil
Coil should be as small as possible consistent with scanning a wide age range 23–44 wk GA
Maximize SNR
Accommodate respiratory aids
Perform accelerated imaging
Easy and safe to position over infants head
2. Positioning
Allow preparation of the neonate away from the scanner with minimal subsequent disturbance
Hold infants in a secure position
Position the head optimally within the coil
Minimise handling of infant during positioning
Facilitate use of life monitoring equipment
Easy access in an emergency
Safe and easy to handle
3. Immobilization
Minimise gross motion of infants head and body
Slim fitting
Comfortable
Accommodate acoustic protection
4. Gradient noise
Reduce startling effects of the scan sequences
Reduce stop-start noise in scan sequences
Attenuate acoustic noise within the bore of the magnet
5. Transport
Transfer infant to scanner bed
Easy to manoeuvre and secure in the stop position
Limited storage space for projectile safety
MR compatible
Assist in keeping the infant asleep

gradient noise throughout the scanning procedure, thereby reducing the disturbing characteristic stop-start noise pattern in conventional MRI protocols. In addition, we also developed robust retrospective motion correction reconstruction techniques to correct for motion artifacts and a restart capability to allow long dMRI scans to be interrupted in order to resettle infants if required without having to restart the whole acquisition (8).

To assess the performance of the new neonatal system, we investigated 1) the SNR gain of the neonatal 32-channel head coil, 2) the number of infants with completed scan protocol, and 3) the number of anatomical images with no motion artifact compared with using the scanner manufacturer supplied adult 32-channel head coil.

Design Considerations

Design of the NBIS involved a number of interacting factors, which were collected together under the following headings: (a) head coil, (b) infant positioning, (c) immobilization, (d) transport, and (e) gradient noise. The detailed design considerations for each of these items are shown in Table 1.

Design Solutions

Neonatal Head Coil

To maximize SNR and support accelerated imaging, the coil should be as close fitting as possible and have as many channels as feasible, while retaining the load-dominated condition (3). Given that infants across a range of postconceptual ages needed to be studied, a key parameter was the maximum head size to be accommodated. We therefore sought a robust estimator of the maximum diametric lengths for the oldest infants in the target age group and adopted the 95th percentile. Measurements were made of anterior–posterior (AP), right–left (RL) and inferior–superior (IS) diameters on previously acquired magnetization-prepared rapid gradient-echo (MPRAGE) brain images on 91 term-born infants (age range at scan, 38.14–44.42 wk. The AP diameter was measured from the nasion to the occiput, on the mid-sagittal slice (Fig. 1a, horizontal blue line). The RL diameter was determined by measuring biparietal diameter at the widest point on the mid coronal view (Fig. 1b, blue arrow) and the IS diameter was measured from the tip of the skull to the body of the third cervical vertebrae on the mid-sagittal slice (Fig. 1a, vertical blue line). The resulting 95th percentile head dimension values taken

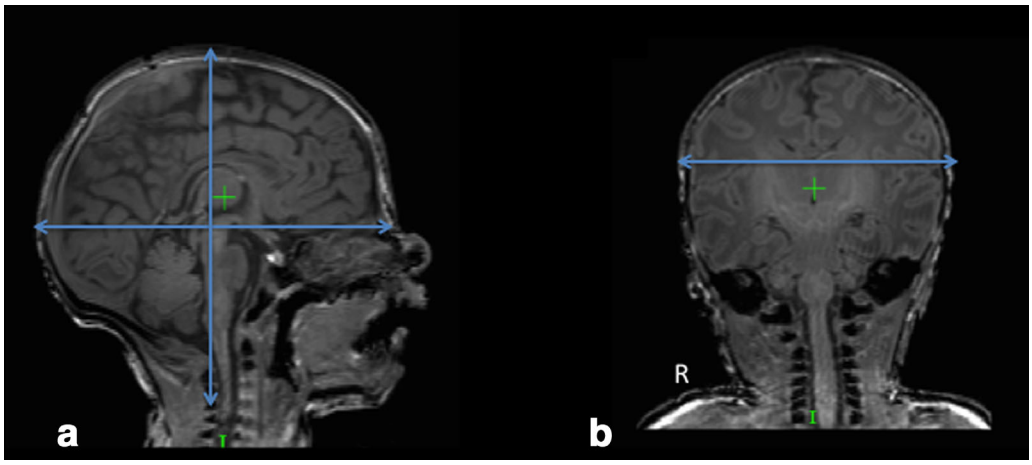

FIG. 1. MPRAGE midsagittal (**a**) and coronal (**b**) views of the neonatal brain. AP measurements were taken from the nasion to the occiput on the midsagittal slice as shown by the horizontal blue line in panel a, and an IS measurement was taken from the top of the skull to the body of the third cervical vertebra as shown by the vertical blue line in the midsagittal slice (a). RL head size was estimated by measuring the biparietal distance (b, blue horizontal line).

for design purposes were: 145 mm (AP) × 120 mm (RL) × 130 mm (IS). Once other design factors relating to coil mechanics and infant handling were considered, the final coil elements were placed on a surface specified with each diameter increased by 10 mm. The final dimensions of the head coil were therefore 155 mm AP, 130 mm RL (Fig. 2b), and 140mm IS (Fig. 2c). The number of channels was set at 32, which was the maximum available on the standard interface of the MRI scanner being used. A 2-cm^2 notch at the coil's open end was added to accommodate respiratory aids (Fig. 2c, green arrow).

Positioning Device

Our previous practice was to start with a sleeping infant, positioned within the adult head coil. Life-monitoring devices (temperature, peripheral oximetry, electrocardiogram, and respiratory monitor) and auditory protection (earplugs molded from a silicone-based putty (President Putty; Coltene/Whaldent, Mahwah, New Jersey, USA) placed in the external auditory meatus and neonatal earmuffs (MiniMuffs; Natus Medical Inc., San Carlos, California, USA) were then applied. No other sound attenuation device, such as an acoustic hood, was used. Swaddling and immobilization of the body was achieved using an air-evacuated beanbag. Foam padding was then placed around the infant's head to prevent gross motion. These elements are essential, but the process was apt to disturb the infant, cause temperature loss during preparation and use up valuable sleep time. For the NBIS, we therefore sought to complete all preparation steps first, away from the MRI suite with the mother, a more favorable condition for settling the infant (1,2). This introduced two challenges: 1) how to achieve the final required position within a small dedicated head coil in the MRI scanner bore and 2) how to ensure safe transport of the finally positioned and immobilized infant.

The solution was a rigid but lightweight protective "shell" (Fig. 2a(iii), 2d) that facilitates infant positioning, allows safe transfer of the infant that docks easily with the head coil (Fig. 2a(i)), and remains at the MRI device. Its purpose is to prepare and securely hold the infant, allowing the user to position the head deep into the head coil with virtually no disturbance to the sleeping infant.

The shell consists of a spheroidal headpiece (Fig. 2e) and v-shaped base section to support the infants' body (Fig. 2d). The headpiece is shaped to precisely match the inner surface of the head coil so that correct positioning within the former guarantees correct positioning within the latter (Fig. 2f). By minimizing the thickness of materials used and using a rail system to achieve precise alignment (Fig. 2g), the distance from the inner surface of the headpiece to the coil elements was kept to <5 mm.

The v-shaped base of the shell starts at 1 cm below the lower inner surface of the headpiece to allow space for a vacuum-evacuated bag filled with polystyrene beads. When finally positioned, the inner surface of the vacuum bag molds to the infant's body, holding it in a fixed position, while the outer surface molds to the v-shaped base, preventing lateral movement of the body independent of the head. To one side of the base there is a dedicated space to secure an oxygen saturation monitor and battery box (Fig. 2d, green arrow). This allows the user to manually lift the infant and shell with vital sign monitoring securely in place.

Once the infant is positioned and secured in the shell, safe handling is achieved by grasping the centrally

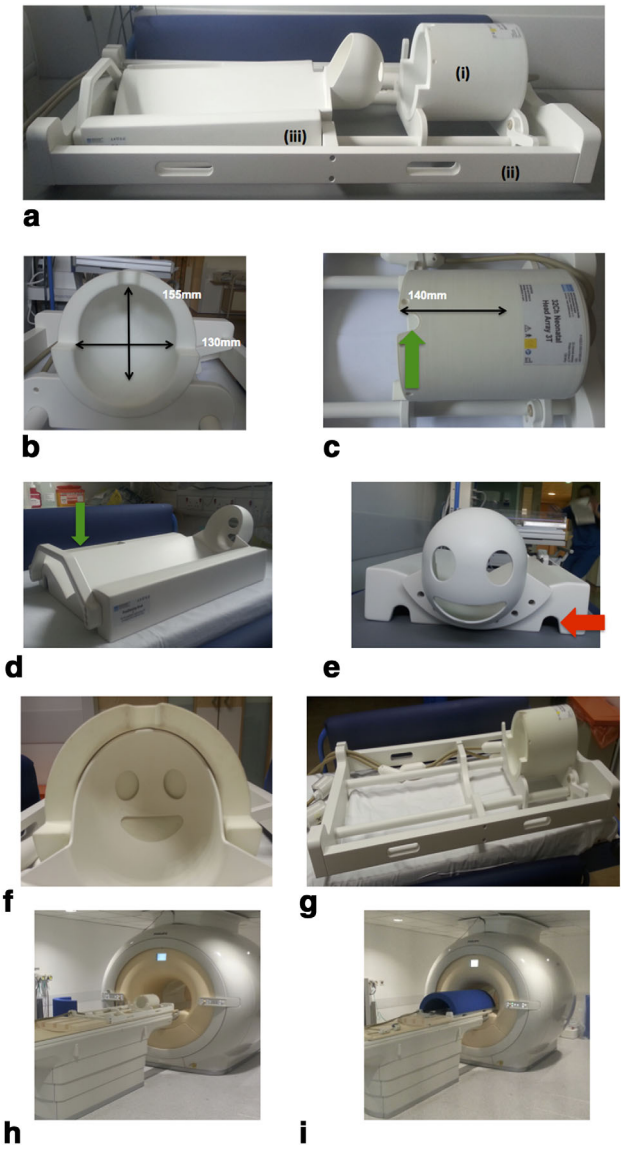

FIG. 2. Three components of the NBIS, consisting of (**a**(i)) the neonatal head coil, (a(ii)) the frame, and (a(iii)) the positioning shell. (**b**) End view of the neonatal head coil showing the AP and RL diameter of the coil (black arrows). (**c**) Top view of the coil. The black arrow denotes the IS length of the coil; the green arrow indicates a 2-cm^2 gap for respiratory aids; (**d**–**f**) Positioning shell, consisting of a v-shaped base and a round headpiece with a pocket for the saturation monitor (d, green arrow). The base of the shell has grooves that allows it to be placed securely on the rails of the frame (e, red arrow). The headpiece has three openings for positioning and viewing the final position of the infant's head (**e**). (**f**) The distance between the headpiece and the coil is <5 mm to preserve SNR. (**h**) NBIS system on the scanner table top. (**i**) Acoustic hood in situ over the NBIS before positioning the infant in the scanner.

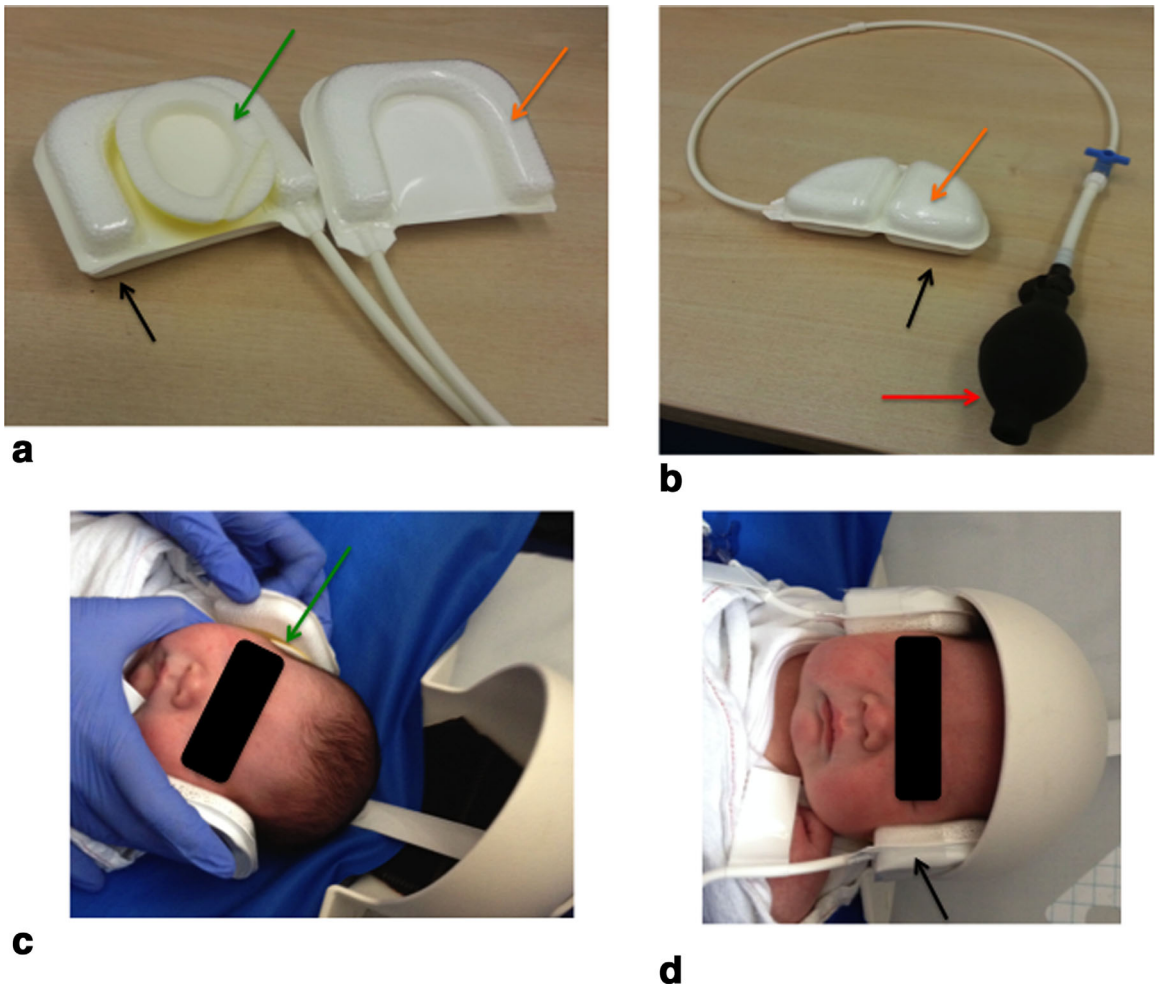

FIG. 3. Specially designed positioning and immobilization devices. (**a, b**) The devices consist of bead-filled cushions (orange arrows) backed by an inflatable air cushion (black arrows). Immobilization devices that sit over the ear muffs (a, green arrow) with an air pump (b, red arrow) allow fine control of head position and comfort. A positioning cushion (b) sits under the base of the neck of the infant. Inflation of this cushion allows fine control of the AP tilt of the infant's head. (**c**) Positioning of the ear immobilizers over the mini-muffs (green arrow). (**d**) Immobilizers in situ with the inflated air pocket (black arrow).

located handlebar at the foot end of the shell and placing a hand under the headpiece, which has an anti-slip matt surface. This allows the user to safely control the infant's head and body within the shell when lifting.

The coil and shell with the infant both sit on a heavy scanning base frame featuring a pair of rods that act as guide rails (Fig. 2g). Handles on either side of the frame allow it to be easily lifted on and off the scanner tabletop. The coil is free to slide along the rails between end stops and can be locked in place with a pair of cam fixings. The coil remains on the frame. The shell is placed onto the rails between its locating end stops. It has slots in its base so that it self-centers when lowered into place (Fig. 2e, red arrow). When in position on the frame, the v-shaped section has a 2° IS incline upward toward the head so that the infant does not lay completely flat, minimizing gastro-esophageal reflux following feeding. All life monitoring can then be connected and checked for correct function. The head coil smoothly slides over the head section of the shell to a final preset fixed location, where it is locked into place. An acoustic hood is then placed over the assembly before the final movement to the magnet isocenter in the scanner bore (Fig. 2i).

Immobilization

Due to the close fitting nature of the headpiece of the shell, foam padding such as that used previously to immobilize the head could not be used. Therefore, specifically designed thin immobilization devices were created to consistently position the head within the headpiece and reduce head motion (Pearltec, Zurich, Switzerland). These devices are made from thin sheets of microbial-resistant thermoplastic polyurethane that satisfy clinical infection control requirements. Each device consists of a bead-filled pad that conforms to the shape of the infants' head (Fig. 3a, orange arrow) backed by an inflatable air pocket (Fig. 3a, 3b, 3d, black arrows) that flexibly fills any remaining gap to the headpiece. These are positioned over the ear acoustic protection (Fig. 3a, 3c, green arrows) to reduce RL motion, and are simultaneously inflated using separate hand pumps (Fig. 3b, red arrow)

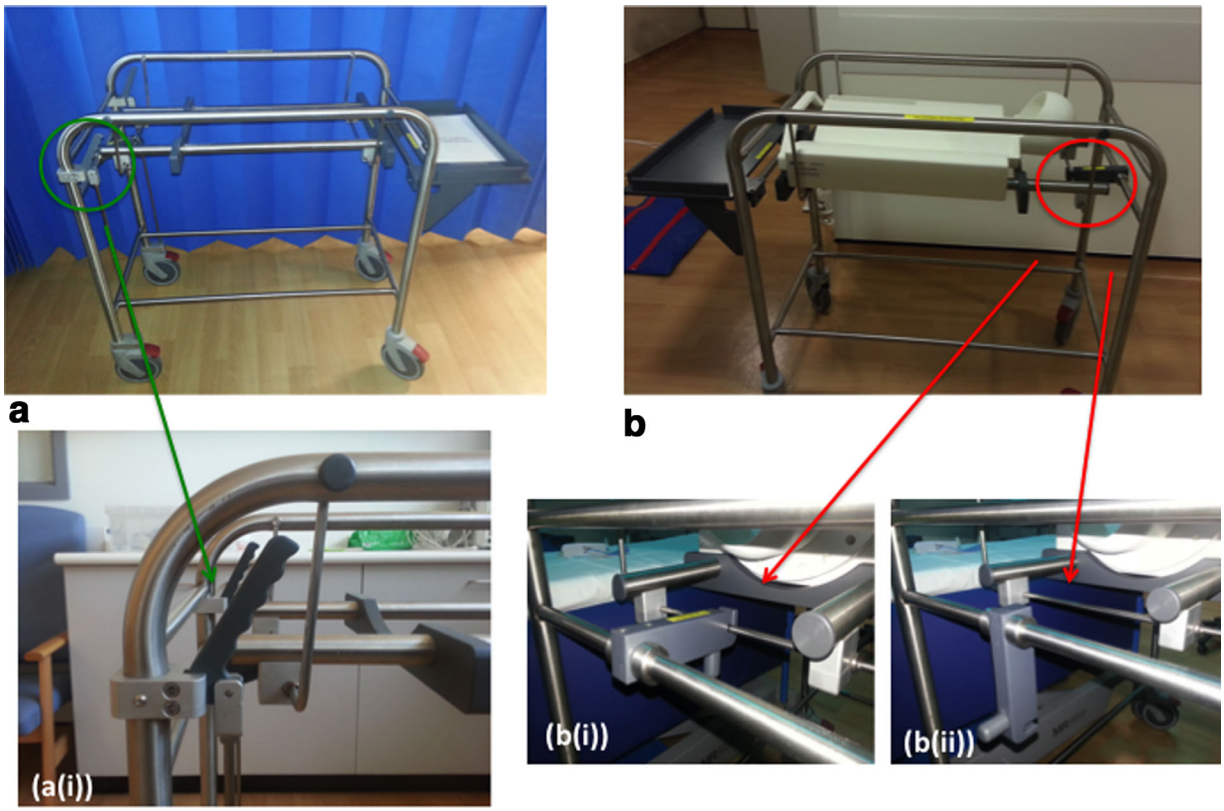

FIG. 4. NBIS MRI-compatible trolley (**a**) with the shell in situ (**b**). (**a**(**i**)) The green circle and green arrow indicate a close-up of the breaking system whereby the trolley can only move once the lever is depressed. The rails on which the shell sits is identical to the rails on the NBIS frame that sits on the scanner bed. The frame can be locked (**b**(**i**)) and unlocked (**b**(**ii**)) to allow the shell to rock backward and forward to settle the infant.

allowing fine control to ensure both immobilization and comfort. The side cushions are 14 mm thick when deflated and can expand to 23 mm. An additional cushion is placed under the shoulders below the base of the neck (Fig. 3b). Inflating this cushion allows the user to change the AP tilt of the head without handling the infant.

Transport

A dedicated MRI compatible trolley was created to transfer the positioning shell with the infant in situ to the MRI scanner bed (Fig. 4a). The skeletal nature of its design ensured that any non-MRI compatible devices placed on the trolley would be clearly visible and identified for removal before entering the magnet room. The trolley has a pair of rails identical to those on the MR scanner table base frame, so that the shell is securely held in place (Fig. 4b), but can be transferred on and off the trolley without disturbing the infant. The rails are held in an articulated structure with a locking mechanism (Fig. 4b(i), 4b(ii)). When locked, the shell is held in a fixed position, but it can be released to allow the shell to be gently rocked forward and backward to pacify the infant. The trolley has soft rubber wheels with brakes that are held locked unless manually released by depressing handles for steering the trolley (Fig. 4a(i)). This ensures that when not in motion, the trolley is in a secure stop position.

Gradient Noise

To avoid sudden sound changes that might disturb the infant's sleep, the MRI scanner software was modified to introduce a user defined start-up period for all scans (Gyrotools, Zurich, Switzerland). During the start-up phase, the sequence gradients are played out repeatedly with amplitude increasing linearly in time from zero to the required operating point. No radiofrequency pulses are applied during this period. Tests performed with pediatric populations have shown that during MRI, a slow ramp-up in acoustic noise is effective at avoiding a startle response (9). In this study, a 5-s ramp-up period was used.

Preparation of the Shell and Infant Positioning

Details of the preparation of the shell are shown in Supporting Video S1. The shell is placed on top of the trolley with an oxygen saturation-monitoring box in situ. A vacuum bag and a neonatal slide sheet are positioned on top of the v-shaped base. A specially designed cotton wrap sheet that contains a pocket extension with a pull tag at the head end is placed on top of the slide sheet. The pull tag is placed through the bottom hole of the headpiece (Fig. 2e). Soft, thin (0.5 cm) foam padding and the neck/shoulder cushion are then placed into the pocket of the wrap sheet.

Before feeding, the infant has cardiac monitoring devices and ear defenses in situ and a fiber optic temperature probe (InVivo, Best, Netherlands) fixed into its axilla with micropore (3M, Maplewood, Minnesota, USA). Once asleep, the infant is then placed on the wrap sheet, with its head placed on the rectangular pocket near the headpiece of the shell. The oxygen saturation probe is attached to the infant's foot. The infant is then wrapped and the immobilization pieces are gently held to the infant's head and is allowed to settle. The infant's head is then glided into the headpiece (Supporting Video S2) by pulling on the tag of the wrap sheet. A second person gently guides the head to ensure it is not bumped. This allows safe positioning with virtually no disturbance to the infant and no stress applied to its neck. The additional holes in the headpiece (Fig. 2e, 2f) allow visual confirmation that the head is positioned as close as possible to the top of the shell headpiece ensuring maximum SNR.

Once the infant's head is in position, the inflatable cushions under the base of the infant's head and over the acoustic ear protection are inflated until the head is in a neutral position so that motion is reduced. The body of the infant is then immobilized by gently wrapping the vacuum bag around the infant and applying suction.

Using the trolley, the infant is then transferred to the scanner bed and the shell with the infant on board is lifted and placed on the frame. The head coil is positioned over the headpiece and secured into place. Once vital sign monitoring is satisfactory, an acoustic hood (Fig. 2i) is placed over the shell and the infant is positioned into the scanner bore.

During the design process of the NBIS, there was also a review of what actions to take in the event that an infant wakes up. Previous practice was to try to resettle the infant by whatever means were appropriate at the time, which could include a gloved fingertip to suck on, or with parental permission, use of a pacifier and sucrose. In some cases the infant was removed from its position and resettled. With NBIS, a much more standard approach has been adopted. If an infant wakes up, the soothing devices described above are given but without any handling of the infant (i.e., the infant remains in situ).

METHODS

The performance of the NBIS was tested against the performance of the conventional infant scanning using the adult head coil and evaluated using the following criteria: 1) differences in SNR, 2) number of infants with a fully completed protocol, and 3) number of images with no motion artifacts on the sagittal MPRAGE and axial T2 turbo spin echo (TSE).

The MPRAGE acquisition parameters used for the adult coil were as follows: pulse repetition time (TR)/echo time (TE) = 17/4.6 ms, inversion time (TI) = 1465 ms, flip angle = 13°, acquired voxel size = 0.82 × 0.93 × 1.0 mm, number of slices = 240, field of view (FOV) = 210 × 157 × 120 mm, time = 7.45 min; parameters used for the neonatal coil were TR/TE = 11/4.6 ms, TI = 713 ms, flip angle = 9, acquired voxel size = 0.8 × 0.8 × 0.8 mm, number of slices = 135, FOV = 145 × 145 × 108 mm, SENSE factor = 1.2, time = 4.35 min. The T2 TSE acquisition parameters used for the adult coil were TR/TE = 14473/160 ms, acquired voxel size = 1.14 × 1.14 × 2 mm, slice gap = −1 mm, TSE factor = 16, number of slices = 92, profile order = linear, sense factor = 2, time- = 3.22 min; parameters used for the neonatal coil were TR/TE = 12,000/156 ms, acquired voxel size = 0.8 × 0.8 × 1.6 mm, slice gap = −0.8 mm, TSE factor = 12, number of slices = 125, profile order = asymmetric, sense factor = 2.1, time = 3.12 min.

All phantom and in vivo imaging was performed on a Philips Achieva 3T magnet at the Evelina Newborn Imaging Center at St. Thomas Hospital (London, UK). Written informed parental consent was obtained prior to scanning.

SNR Gain

SNR Evaluation: Phantom

An experiment was performed to assess the possible SNR gain of the 32-channel neonatal coil compared with a 32-channel adult receive array (Philips, Best, Netherlands). Both coils were used to scan a dedicated phantom designed to fit the neonatal coil. The phantom was 3D-printed from nylon using selective laser sintering and was formed from two halves, each of which included a threaded section, so that they could be screwed together and glued to achieve a water-tight join. A filling spout at the top could be plugged with a rubber bung containing an injection membrane for final top-up using a syringe. Its outer shape matched the headpiece of the shell. It had 10-mm-thick walls, and the interior surface was varnished to ensure water-tightness (Fig. 5(iii)). The phantom was filled with physiological saline (0.9%), doped with Gadovist to achieve a T1 of approximately 300 ms. For SNR evaluation of the adult coil, the phantom was placed in its geometrical center, supported by foam padding.

A 3D spoiled gradient echo sequence was acquired (FOV = 140 × 140 × 140 mm, resolution = 1 × 1 × 1 mm, TE = 6 ms, TR = 30 ms, flip angle = 30°, bandwidth = 200 Hz/pixel). The raw k-space data were exported and reconstructed offline. Individual complex images for each coil element were reconstructed by simple Fourier transform and combined by taking the sum-of-squares. SNR maps were created by dividing the sum-of-squares image by the average of the noise signal in a background region of interest. This process was repeated for both coils. A correction factor may be applied to the mean of the absolute noise signal to convert this to the standard deviation of the unrectified noise, but this was not applied, because it was common to both measurements being compared.

SNR Evaluation: Infant Brain

In vivo evaluation of SNR was obtained by performing a dMRI acquisition (TR = 7856 ms, TE = 49 ms, voxel size = 2 × 2 × 2 mm, FOV = 224 × 224 × 98 mm, number of directions = 32, maximum b factor = 750 s/mm^2) on two infants. The first infant was imaged at 44 + 3 wk PCA, age at birth 40 + 1 wk using the 32-channel adult head coil, and the second infant was imaged at 43 + 2 wk PCA, age at

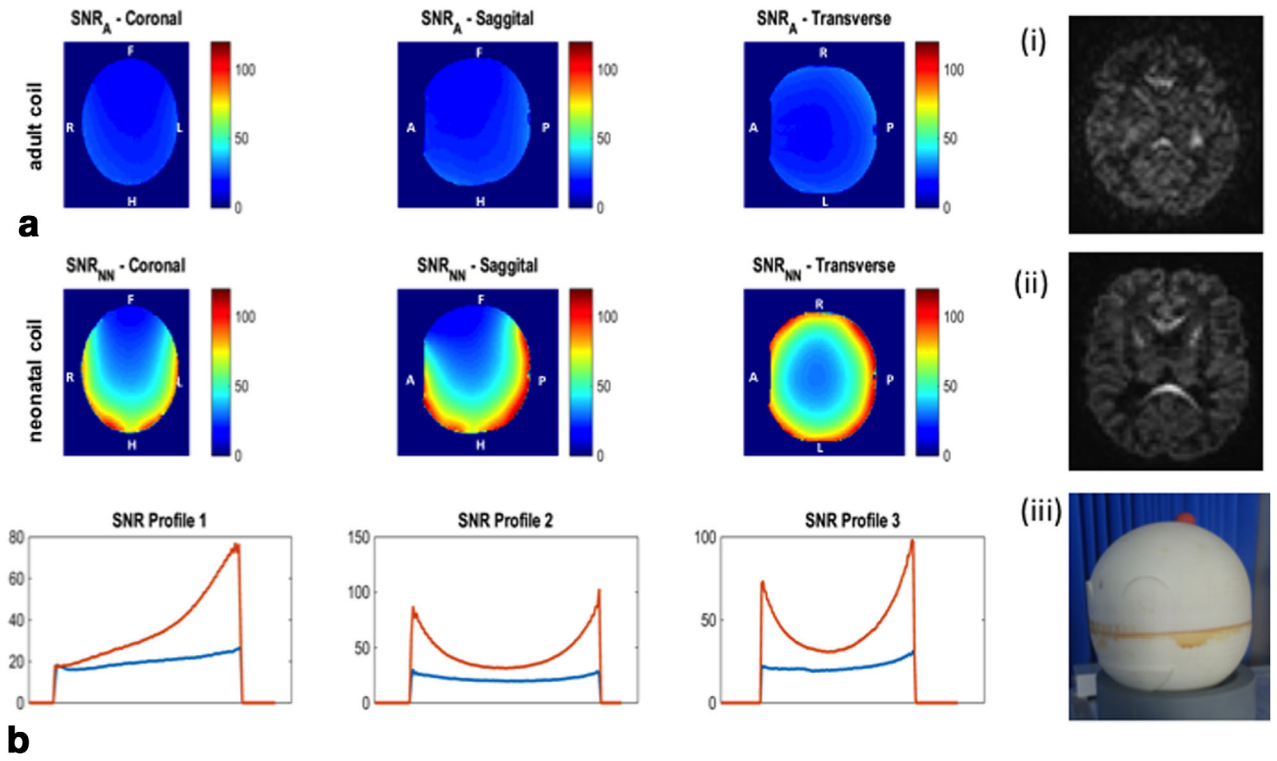

FIG. 5. (**a**) Uniform SNR for a phantom in the adult coil. (**b**) Enhanced SNR results for the phantom in the neonatal coil. (**i, ii**) The SNR gain is evident in DTI images performed in term babies with greater contrast-to-noise ratio in the cortex for the infant imaged in the neonatal coil (ii) compared with the adult coil (i). (**iii**) Image of the phantom used to assess the SNR in each coil. A, anterior; I, inferior; L, left; P, posterior, R, right.

birth 41 + 2 wk using the 32-channel neonatal coil. The SNR in both data sets were ascertained using Image J software v1.49 (National Institutes of Health, Bethesda, Maryland, USA). A mask of the B0 image was created and the mean and standard deviation of the signal across all volumes in both dMRI data sets was estimated.

Acoustic Noise Attenuation

Infants scanned using the adult coil and the NBIS both had the same ear protection described previously. However, for NBIS we employed an acoustic hood. We were not able to reliably compare measurements of the noise attenuation for the NBIS and the adult coil because precise results depend heavily on consistency of the microphone position. We therefore measured the sound attenuation with and without the hood as a function of frequency. The test was performed using the DHCP multiband (MB) functional MRI (fMRI) sequence, because it has more consistent nonvarying noise levels. A Castle GA221 MR-compatible microphone (Castle Group Ltd, Scarborough, UK) was placed pointing in an RL orientation at the isocenter of the magnet and at the center of the hood. The level of noise (dBA) generated at each octave band was measured for the open bore and with the hood in situ.

MR Protocol Completion and Motion Artifacts

A retrospective assessment was performed on infants imaged previously using the 32- channel adult head coil and with the new neonatal system.

Subjects

Adult Coil

From December 18, 2013, until November 17, 2014, 243 infants underwent an MRI of the brain using a Philips 32-channel adult head coil. Only term-born infants who underwent imaging without sedation were included in the analysis (n = 68). Infants were positioned in the adult head coil and were monitored and immobilized as described previously. Once in position, and once vital sign monitoring was stable, the MRI scan protocol was started (Table 2). The number of infants with a completed MRI protocol and images with no overt motion artifacts was ascertained.

NBIS with Dedicated Neonatal Coil

Between February 6, 2015, and November 17, 2015, 171 infants underwent brain MRI using the NBIS. Only term-born infants imaged without sedation were included in the analysis (n = 132). The infants were prepared as described in the "Preparation of the Shell and Infant Positioning" section in this article. The number of infants with a completed full MRI protocol and images with no overt motion artifacts was ascertained.

Imaging

The MRI protocol and the time taken to perform each sequence on each coil are shown in Table 2.

Table 2
MRI Protocol and Cumulative Time Taken to Perform Each Sequence on the Adult Coil and the Neonatal Coil

	Time from Start of Examination
Adult coil	
Pilot	00:00:0
Reference	00:00:31
T2 TSE axial	00:01:05
MP-RAGE sagittal	00:04:27
DTI shell 1	00:12:08
B0_PA	00:17:49
DTI shell 2	00:18:43
rsfMRI	00:32:31
End time	00:39:04
Neonatal coil	
Pilot	00:00:00
reference	00:01:00
B0 map	00:01:25
B1	00:01:45
T2 TSE axial	00:01:49
MP-RAGE sagittal	00:05:01
T2 TSE sagittal	00:09:36
SE_fMRI	00:12:48
SB_fMRI	00:14:00
MB_fMRI	00:14:19
SB_fMRI_rep	00:29:23
SB_DTI	00:29:42
MB_DTI	00:31:31
B0_shim_map	00:50:51
T1_TSE_IR_axial	00:51:11
T1_TSE_IR_sagittal	00:56:56
End time	01:03:13

Abbreviations: B0_PA, reversed-phase encoded B0; DTI, diffusion tensor imaging; IR, inversion recovery; rsfMRI, resting state functional MRI; SB, single band; SE_fMRI, spin echo functional MRI.

Assessment of Motion

Motion on T2 TSE axial and sagittal MPRAGE data was assessed by an experienced radiographer using RView image display software (https://biomedia.doc.ic.ac.uk/software/). Visual inspection was performed on the images in the native and orthogonal planes. Small and gross motion artifacts were detected by observing disrupted slices in the orthogonal views for the T2 TSE axial (Fig. 6) and motion artifacts on the MPRAGE. Only images with no disrupted slices visible in any plane were regarded as having no motion.

RESULTS

The design outlined above resulted in a coil and infant handling specification that was built by Rapid Biomedical (Rimpar, Germany). The coil was tested by Rapid Biomedical for safety, including radiofrequency safety modeling and was CE (Conformité Européene) marked.

SNR Evaluation

The results of the phantom SNR experiments are shown in Fig. 5. The SNR of the adult coil is relatively uniform across the phantom compared with the neonatal coil, which shows greatly enhanced SNR local to the receive elements, with a maximum enhancement factor of approximately 4. In the center of the phantom, the SNR enhancement is approximately 1.5. Averaged across the whole phantom the SNR is improved by a factor of 2.4.

A typical dMRI using the neonatal head coil compared to the adult head coil is shown in Fig. 5. A 1.55 factor increase in SNR was seen using the neonatal coil and as a result, greater contrast between the gray/white matter border was more visible in the acquired images.

Acoustic Noise Attenuation Evaluation

The acoustic hood produced an overall reduction in noise level of 10.6 dBA at a midrange frequency of 1 kHz, with a maximum attenuation of 17.5 dBA at the higher frequency of 4 kHz. A graph showing the noise level at different octaves with and without the hood and the total attenuation provided by the hood can be seen in Supporting Figures S1a and S1b, respectively.

Performance of the NBIS

Of the 132 infants (median $40+2$ wk PCA at scan; age range, $36+5$ to $43+3$ wk) included for analysis, three parents requested that scanning be stopped before completion of the protocol due to their own anxiety. Scanning was stopped on two occasions due to incidental findings that required more detailed clinical examination. A further two studies were incomplete due to technical errors. Hence, a total of 125 term-born unsedated infants had MRI research scans that were not interrupted due to outside influences. Of these, 36 infants awoke during scanning, but 24 of these were resettled and the protocol was completed. Interrupted scans in all cases were repeated. This yielded a total of 113 (90%) term-born infants that successfully completed the scanning protocol using the NBIS.

All 132 infants underwent both MPRAGE and T2 TSE imaging. No motion was evident on 58 (44%) MPRAGE images and 70 (53%) T2 TSE images.

Performance of Imaging on the Adult Head Coil

Of the 68 infants imaged without sedation (median $41+1$ wk PCA at scan; age range, $37+2$ to $46+4$ wk), one scan was stopped before completion at the parents' request. Thirty-six infants woke up during the scanning protocol, two of whom were resettled and the protocol completed. This yielded a total of 34 infants out of 67 (51%) who completed the imaging protocol. The average PCA at scan on the adult coil ($41+4$ wk), was significantly higher than the average age at scan for NBIS ($40+4$ wk).

All 68 infants had MPRAGE and T2 TSE imaging. No motion was detected on 30 (44%) of MPRAGE images and 34 (50%) of the T2 TSE images.

A graphical summary of the performance of the NBIS compared with the adult head coil can be seen in Fig. 7.

DISCUSSION

The goal of the DHCP is to acquire high-quality structural MRI, fMRI, and dMRI to create the first four-dimensional connectome of the brain in the critical period of brain development. These subjects constitute a vulnerable cohort for which MRI of the brain presents a

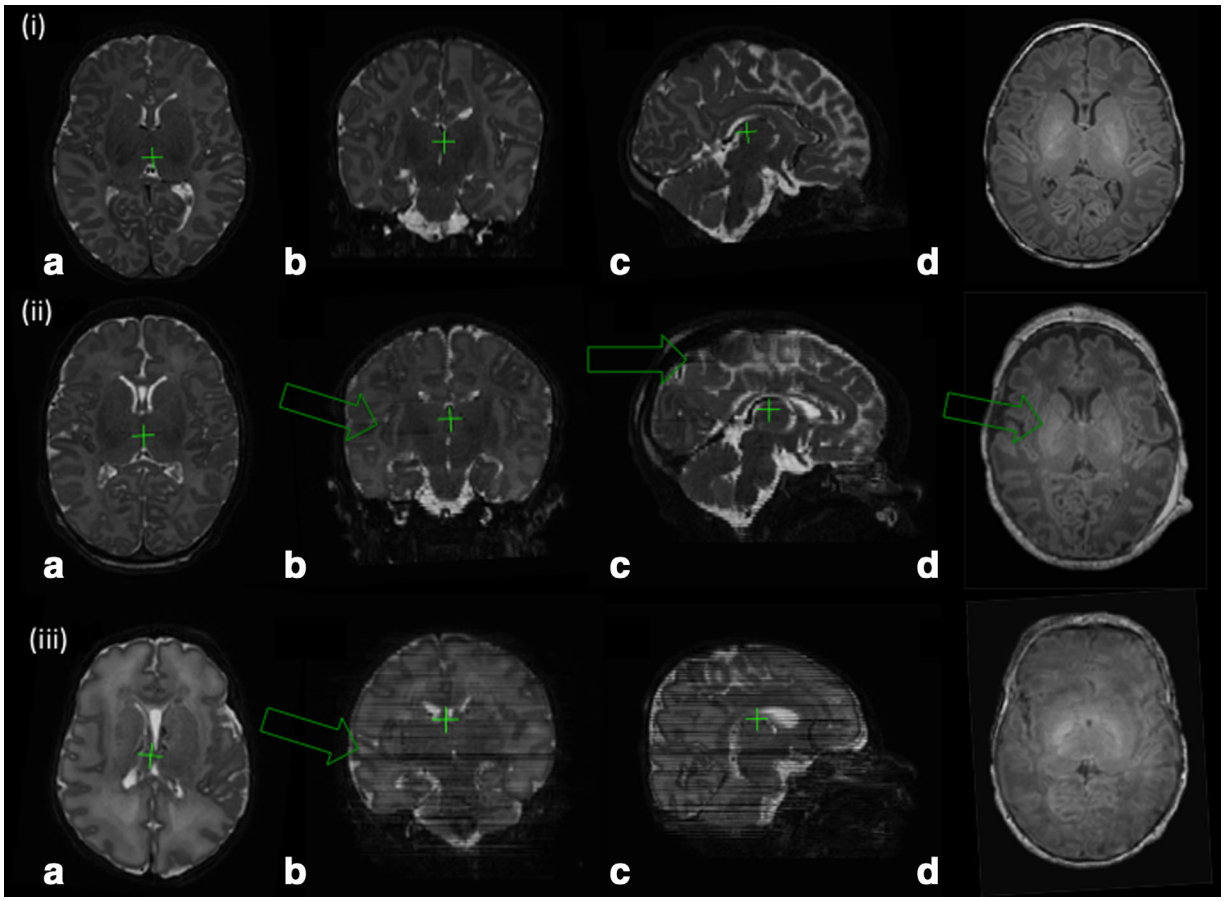

FIG. 6. Three examples of axial T2 TSE and MPRAGE images uploaded on RView. Example (**i**) shows no evidence of motion on the acquired T2 axial (i)(a), and there are no disrupted slices in the two orthogonal T2 planes (i)(b) and (i)(c). These images were determined to have no motion. Example (**ii**) had evidence of minor motion artifact present on the coronal (ii)(b) and sagittal planes (ii)(c). Example (**iii**) had gross motion artifact on the coronal and sagittal planes (iii)(b) and (iii)(c) and axial MPRAGE (iii)(d). Motion evidenced by disrupted slices in the T2 orthogonal views are indicated by the green arrows. Example of no motion on MPRAGE were as in example (i)(d), moderate motion in row (ii)(d), and gross motion in row (iii)(d).

number of technical and practical challenges. We specifically designed an NBIS consisting of a joint design of a close-fitting 32-channel phased array coil and a positioning device to fulfill the aims of the DHCP. The coil delivers approximately double the SNR averaged over the neonatal brain volume compared with the standard adult 32-channel head coil. The positioning system allows for both consistent placement of the infants' head deep into the head coil to gain maximum SNR benefit, and enhanced infant preparation capabilities. When compared with the traditionally used arrangement involving the adult head coil, the NBIS provides a substantially increased completion rate of the imaging protocol, as well as a decreased number of disturbances related to the infant waking up during the scan procedure.

Close-fitting receive array coils have demonstrated superior SNR gain for pediatric imaging compared with adult head coils (3). The performance of our neonatal 32-channel receive array coil was consistent with this earlier result, with an average SNR gain factor of 2.4 compared with the adult coil and the greatest SNR gain factor of approximately 4 in regions closest to the receive elements. The benefits of improved SNR are numerous in neonatal/infant MRI and include the ability to acquire

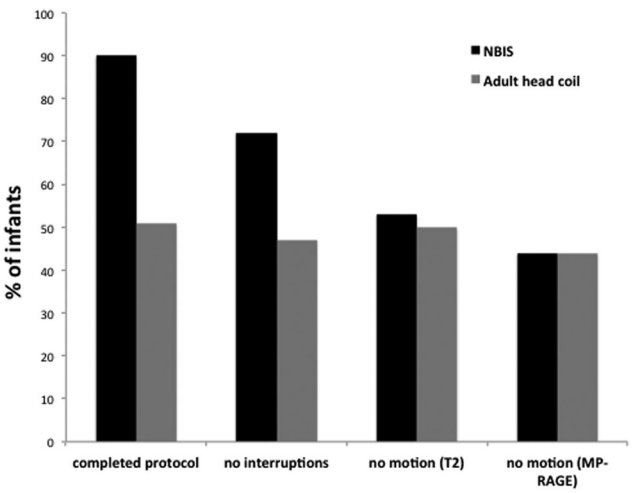

FIG. 7. Performance of the NBIS compared with the adult head coil. The neonatal system had a greater number of infants with a completed protocol and fewer interruptions due to the infant waking than using the adult coil. There was little to no difference in the number of images with evidence of motion artifact on T2 TSE and MPRAGE images.

anatomical sequences at higher resolution (0.8 mm^3), the reduction of partial voluming effects (10) allowing improved anatomical segmentation (11,12), and an improved sensitivity profile that allows more robust motion correction techniques to be employed (13,14). In addition, echo planar imaging (EPI) sequences such as those used for dMRI and fMRI can be accelerated significantly using simultaneous multislice methods (15–18) with higher multiband (MB) factors as unfolding of aliased slices depends on localized coil sensitivities (19,20). The DHCP EPI protocol uses MB factor 9 for fMRI (20) and MB factor 4 for dMRI (8). In addition, for dMRI it permits the use of high b-values for improved characterization of the movement of water with high angular resolution to better delineate crossing white matter fibers in the brain (8).

The benefits of using a close-fitting receiver coil are inevitably accompanied by practical challenges. Positioning the head of a sleeping infant deep into the neonatal head coil required careful design consideration. The performance results for the neonatal system show that over 70% of scans during the DHCP protocol are performed with no disturbance to the infant, and 90% of the infants completed the full imaging protocol. This was a substantial improvement over our previous imaging protocol in unsedated infants performed on an adult head coil. We attribute this increase in success rate to our strategy of allowing the infant to fall asleep under more favorable circumstances and minimizing the amount of disturbance prior to commencing the scanning protocol. The "shell" with the immobilization devices allows final positioning with the minimum amount of handling. Early settling of infants before the start of the scan is consistent with that reported in other studies (1,21). We found that over half the unsedated term-born neonates woke up one or more times during the MRI procedure before implementation of the NBIS. Other studies that followed a similar protocol for infant preparation also found that nearly half of unsedated infants wake up during the MRI protocol (2), with shorter clinical studies reporting approximately 30% disturbance (22).

In this study, we combined minimal handling and preparation outside the scanner with a slow ramp-up in scanner noise and an acoustic hood designed to reduce acoustic disturbances. Noise that abruptly changes in sound level or intensity in a nonprogressive manner is much more likely to result in arousal and waking (9). This effect is far more obvious when there is a change from silence to noise, as only two infants in the study awoke after a scan was completed; all others ($n = 34$) woke up at some point during the scan. During initial testing, slow ramping of the gradients appeared to markedly reduce the startle responses associated with the sudden sound level changes during conventional start/stop MRI examinations. However, we have not performed group studies in which the contributions from gradient ramping and the NBIS preparation process were separated, thus we can only conclude that their combination was highly effective in increasing the successful rate of completed scan protocols in longer research -based MRI protocols, without being able to attribute specific benefits to the two elements.

There is a distinction between keeping the infant asleep so that the imaging examination can run to completion and the risk of movements during natural sleep, which will produce motion artifacts. Although the scan protocol completion rate was significantly increased with the NBIS, the number of images with movement artifacts did not significantly differ from imaging performed on the adult head coil. Approximately 50% of structural images had motion artifacts. A similar study also found that unsedated neonatal MRI brain scans ($n = 152$) with motion attenuation devices resulted in approximately 50% of scans with excellent quality with respect to motion artifact (21). Immobilization of the infant's head cannot be too restrictive, because this will become uncomfortable for the infant, who may become distressed and awaken sooner. These results suggest that motion during natural sleep in infants is a characteristic feature for neonatal imaging and necessary for continuing comfort throughout the scan. The immobilization therefore serves to restrict gross motion and changes in global positioning of the head while allowing some motion in order to maintain comfort.

Addressing motion by repeat imaging is time-consuming and runs the risk of termination of the protocol due to time constraints and the infant waking up. Neonatal protocols can thus benefit hugely from robust motion correction methods that result in artifact-free images without scan repeats. Prospective movement detection using optical or other methods would be possible but is challenging when a close-fitting receiver coil is used, and many such systems also require markers to be affixed to the face (23). Prospective methods that do not require external markers use navigators (24). These methods require changes to the sequence structure that can decrease efficiency and also add complexity. For the DHCP, a retrospective data-driven approach has been adopted that exploits the highly localized properties of the individual coil elements in the neonatal coil to achieve estimates of positional change that are then corrected (13). Using this approach, it has been possible to recover virtually artifact-free images from all the anatomical scans that ran to completion.

CONCLUSION

The dedicated neonatal system described here has allowed advanced neonatal brain imaging with high protocol completion rates for the DHCP. The system makes it possible to push the technical boundaries of MRI in the neonatal brain to attain high-resolution anatomical as well high MB factor EPI sequences, which were not previously achievable in neonatal imaging. The positioning system allows us to exploit the SNR gain capability and demonstrates substantial benefits for imaging neonates in natural sleep by minimizing handling and reducing the startling effect associated with the start of scan sequences. When combined with retrospective motion correction to eliminate scan repeats, it has been possible to achieve near-perfect success rates with artifact-free images. The system is now being applied to a much wider range of neonatal brain imaging studies.

ACKNOWLEDGMENTS

This research has received funding from the European Research Council under the European Union's Seventh Framework Programme (*FP7/2007-2013*)/ERC *grant agreement* n° 319456.

REFERENCES

1. Mathur AM, Neil JJ, McKinstry RC, Inder TE. Transport, monitoring, and successful brain MR imaging in unsedated neonates. Pediatr Radiol 2008;38:260–264.
2. Ureta-Velasco N, Martinez-de Aragon A, Moral-Pumarega MT, Nunez-Enamorado N, Bergon-Sendin E, Pallas-Alonso CR. Magnetic resonance imaging without sedation in neonates [in Spanish]. An Pediatr (Barc) 2015;82:354–359.
3. Keil B, Alagappan V, Mareyam A, et al. Size-optimized 32-channel brain arrays for 3T pediatric imaging. Magn Reson Med 2011;66: 1777–1787.
4. Tocchio S, Kline-Fath B, Kanal E, Schmithorst VJ, Panigrahy A. MRI evaluation and safety in the developing brain. Semin Perinatol 2015; 39:73–104.
5. Golan A, Marco R, Raz H, Shany E. Imaging in the newborn: infant immobilizer obviates the need for anesthesia. Isr Med Assoc J 2011; 13:663–665.
6. Edwards AD, Arthurs OJ. Paediatric MRI under sedation: is it necessary?. What is the evidence for the alternatives? Pediatr Radiol 2011; 41:1353–1364.
7. Rutherford M, Malamateniou C, Zeka J, Counsell S. MR imaging of the neonatal brain at 3 Tesla. Eur J Paediatr Neurol 2004;8:281–289.
8. Hutter JT, Tournier DJ, Price AN, et al. Optimized Multi-Shell HARDI Acquisition with Alternating Phase Encoding Directions for Neonatal dMRI. In Proceedings of the 23rd Annual Meeting of ISMRM, Toronto, Canada, 2015. p. 3460.
9. Raschle N, Zuk J, Ortiz-Mantilla S, Sliva DD, Franceschi A, Grant PE, Benasich AA, Gaab N. Pediatric neuroimaging in early childhood and infancy: challenges and practical guidelines. Ann N Y Acad Sci 2012; 1252:43–50.
10. Baert AL, Knauth M, Sartor K. Parallel imaging in clinical MR applications. Schoenberg SO, Dietrich O, Reiser MF, editors. Berlin, Heidelberg, Germany: Springer-Verlag; 2007.
11. Robinson EF, Bozek J, Makropoulos A, et al. Quantifying Development of Neonatal Brain Function. In Proceedings of the 22nd Annual Meeting of the Organization for Human Brain Mapping, Geneva, Switzerland, 2016. Abstract 3985.
12. Bozek JB, Makropoulos A, Wright R, et al. In-Vivo Cortical Myelination of the Neonatal Brain in the Developing Human Connectome Project. In Proceedings of the 22nd Annual Meeting of the Organization for Human Brain Mapping, Geneva, Switzerland, 2016. Abstract 4201.
13. Cordero-Grande L, Hughes EJ, Price AN, Hutter J, Edwards AD, Hajnal JV. 3D Motion Corrected SENSE Reconstruction for Multislice MRI. In Proceedings of the 24th Annual Meeting of ISMRM, Singapore, 2016. Abstract 1096.
14. Cordero-Grande L, Teixera, RPAG, Hughes EJ, Hutter J, Price AN, Hajnal JV. Sensitivity encoding for aligned multishot multislice MRI. IEEE Trans Comput Imaging 2016;2:266–280.
15. Barth M, Breuer F, Koopmans PJ, Norris DG, Poser BA. Simultaneous multislice (SMS) imaging techniques. Magn Reson Med 2016;75:63–81.
16. Feinberg DA, Setsompop K. Ultra-fast MRI of the human brain with simultaneous multi-slice imaging. J Magn Reson 2013;229:90–100.
17. Larkman DJ, Hajnal JV, Herlihy AH, Coutts GA, Young IR, Ehnholm G. Use of multicoil arrays for separation of signal from multiple slices simultaneously excited. J Magn Reson Imaging 2001;13: 313–317.
18. Setsompop K, Gagoski BA, Polimeni JR, Witzel T, Wedeen VJ, Wald LL. Blipped-controlled aliasing in parallel imaging for simultaneous multislice echo planar imaging with reduced g-factor penalty. Magn Reson Med 2012;67:1210–1224.
19. Cordero-Grande L, Price AN, Hutter J, Hughes EJ, Hajnal JV. Comprehensive CG-SENSE Reconstruction of SMS-EPI. In Proceedings of the 24th Annual Meeting of ISMRM, Singapore, 2016. Abstract 3239.
20. Price AN, Cordero-Grande L, Malik S, Abaei M, Arichi T, Hughes EJ, Rueckert D, Edwards AD, Hajnal JV. Accelerated Neonatal fMRI Using Multiband EPI. In Proceedings of the 23rd Annual Meeting of ISMRM, Toronto, Canada, 2015. p. 3911.
21. Haney B, Reavey D, Atchison L, Poull J, Dryer L, Anderson B, Sandritter T, Pallotto E. Magnetic resonance imaging studies without sedation in the neonatal intensive care unit: safe and efficient. J Perinat Neonatal Nurs 2010;24:256–266.
22. Neubauer V, Griesmaier E, Baumgartner K, Mallouhi A, Keller M, Kiechl-Kohlendorfer U. Feasibility of cerebral MRI in non-sedated preterm-born infants at term-equivalent age: report of a single centre. Acta Paediatr 2011;100:1544–1547.
23. Maclaren J, Herbst M, Speck O, Zaitsev M. Prospective motion correction in brain imaging: a review. Magn Reson Med 2013;69:621–636.
24. Tisdall MD, Reuter M, Qureshi A, Buckner RL, Fischl B, van der Kouwe AJ. Prospective motion correction with volumetric navigators (vNavs) reduces the bias and variance in brain morphometry induced by subject motion. NeuroImage 2016;127:11–22.

SUPPORTING INFORMATION

Additional Supporting Information may be found in the online version of this article.

Fig. S1. Estimation of noise levels (dBA) with and without the acoustic hood during a multiband fMRI sequence for the DHCP. (**a**) Noise level (in dBA) generated at each frequency with (red) and without (blue) the acoustic hood. (**b**) Total attenuation in noise for each octave provided by the hood.

Video S1. Movie demonstrating the equipment and procedure used to prepare the positioning shell for receiving an infant.

Video S2. Movie showing a term-born, naturally sleeping infant being positioned in the shell before being transported to the MR scanner.